Sensor-based Formation Control of Autonomous Underwater Vehicles

Pedro Caldeira Abreu

Instituto Superior Técnico - Institute for Systems and Robotics (IST-ISR)
Lisbon, Portugal

December 2014

***Abstract*—We address the subject of formation control of underwater vehicles, using either inter-vehicle relative position measurements or range-only measurements. The work is motivated by the MORPH project, aiming to use formations of vehicles with complementary capabilities to map the underwater environment in challenging conditions. The main problem studied is that of driving a vehicle (follower) to an appropriately defined position with respect to another vehicle (leader), which moves along an unknown trajectory. This control task is divided into two steps. Firstly, a trajectory-tracking controller is designed, so that a follower vehicle can track a specified virtual target. Conditions under which the tracking error remains bounded are derived using tools from nonlinear systems theory. Secondly, we design path-generators that provide the position and velocity of the virtual target to be tracked, for both the relative position measurements and the range-only measurements scenarios. These path-generation strategies take into account the formation objectives, typical maneuver geometries and limitations of underwater inter-vehicle communications. Applications envisioned in the scope of the MORPH project are presented and discussed. The implementation of the strategies proposed for formation control with relative position measurements is described, taking explicitly into account the filter architectures required for relative vehicle navigation. Finally, results of simulations and sea trials are shown, with position errors generally below 1 m in MORPH trials in Lisbon and the Azores.**

***Index Terms*—Autonomous marine vehicles, formation control, leader-follower formation, trajectory-tracking.**

I. Introduction

Within the framework of cooperation of marine robots for the purpose of ocean exploration, namely mapping and surveying the seabed, some difficulties arise. Scientifically interesting areas, from geological or biological standpoints, usually occur in challenging, unstructured environments with rough terrain. In these conditions, dead-reckoning navigation instruments like the Doppler Velocity Log (DVL) can provide unreliable results. The idea of using formations of Autonomous Underwater Vehicles (AUVs) with complementary capabilities arises as a possible solution to the problem of operating effectively in challenging environments. The MORPH project (marine robotic system of self-organizing, logically linked physical nodes) [1] brings together a consortium involving multiple partners from both the industry and academia. It proposes the concept of a physically morphing structure composed of robotic vehicles with complementary capabilities, linked by acoustic communication channels. The formation consists of the Surface Support Vehicle (SSV) used for global navigation, the Global Communications Vehicle (GCV) responsible for maintaining the accuracy of inter-vehicle navigation and communications, the Local Sonar Vehicle (LSV) carrying a multibeam echosounder for mapping the terrain, and two camera vehicles C1V and C2V which carry onboard cameras. The first three vehicles compose the *upper segment*, while the two camera vehicles are part of the *lower segment*. The system should not depend on any direct communication between the SSV and any vehicle other than the GCV, since the geometry of the environment may block these acoustic links. Figure 1 shows the structure of the MORPH system when mapping a flat seabed and a negative slope wall. Clearly, effective formation keeping is instrumental in controlling the motion of the robotic nodes in such a system.

In this context, the problem of formation control of underwater vehicles is studied, with emphasis on applications to the MORPH project. The underlying problem can be broadly described as deriving control laws so as to drive a vehicle (follower) to an appropriate position relative to another vehicle (leader), using either relative position measurements or range-only measurements between the vehicles. The trajectory of the leader is unknown a-priori by the follower. Applicability to MORPH implies that aspects such as typical mission geometries and practical limitations of onboard sensors and acoustic underwater systems, used for both communication and positioning, should be considered when defining the desired behaviour of the formation.

In the last decades the problem of motion control of marine vehicles has received considerable attention, with AUVs and ROVs becoming increasingly commonplace for a number of scientific and industrial purposes. Specifically, the problems of trajectory-tracking (TT) and path-following (PF) are widely covered in the literature. Both consist of forcing a vehicle to track a desired trajectory, the difference being that the former imposes a timing law while the latter prescribes only a desired speed profile. In [2], the authors study these problems for the case of underactuated autonomous vehicles, proposing full-state feedback controllers that drive the tracking error to an arbitrarily small neighborhood of the origin. Trajectory-

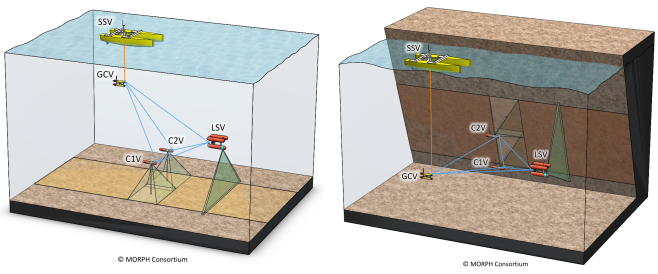

Figure 1: Structure of MORPH in two scenarios [1].

tracking techniques are instrumental in this paper, since they will be used to force each vehicle to track an appropriately defined virtual target. For the problem of controlling formations of vehicles, a number of techniques are reported in the literature. If the paths are known a-priori by all the vehicles, we call the problem cooperative path-following (CPF) [3]. If the path is not known a-priori, possible techniques for formation-keeping include, among others, the potential field approach [4], Model Predictive Control (MPC) optimization-based methods [5], the virtual structure method, and the leader-follower approach [6], which despite over-reliance on a single vehicle is very appreciated for its simplicity and scalability. The particularities of the marine environment preclude techniques that require heavy inter-vehicle communication from being used for formation control, further increasing the relevance of keeping the formation strategies simple. For these reasons, in this paper we resort to leader-follower formation techniques. Regarding the MORPH project, previous work focuses specifically on formation control using range-only measurements [7], [8], [9], [10], which is used only by the lower segment vehicles.

The main contributions of this thesis are threefold. Firstly, the trajectory-tracking problem is studied in a decoupled inner-outer-loop control architecture, which leads to more intuitive control laws. Sufficient conditions for boundedness of the tracking error are derived, considering estimation errors explicitly. Secondly, leader-follower formation control is achieved in both the relative position and range-only measurement scenarios by designing a path-generator block, which creates a virtual target to be tracked by the trajectory-tracking controller. The proposed path-generators take into account typical mission geometries and attempt to keep inter-vehicle communication to a minimum. Thirdly, an information flow strategy is proposed, the controllers are adapted, and estimators are introduced to allow implementation in MORPH. Results were obtained in sea trials for upper segment follower vehicles, with formation errors generally under 1 m.

The remainder of this paper is organized as follows: Section 2 briefly introduces nomenclature and the AUV model used throughout the paper; Section 3 addresses the problem of trajectory-tracking; in Section 4, we study the design of path-generators that generate a virtual target so as to achieve the desired formation; Section 5 describes in broad terms the implementation of the proposed controllers in the MORPH vehicles; Section 6 evaluates the work in previous chapters with results from computer simulations and sea trials; Section 7 contains concluding remarks and points towards possible directions of future research.

II. AUV Dynamics

A. Reference frames and naming conventions

Following usual practice, we define both a body-fixed frame, in which the dynamics of the vehicle are more conveniently described, and an earth-fixed frame, with respect to which the position and orientation of the vehicle are described. The body-fixed frame $\{\mathcal{B}\}$ is a right-handed, rectangular coordinate system. Its origin O is chosen to coincide with the center of gravity (CG) of the vehicle. Its axes $\{x_B, y_B, z_B\}$ are defined in accordance with the SNAME notation [12], and coincide with the principal axes of inertia at O. We define a *flat Earth navigation* frame $\{\mathcal{I}\}$. This is a local NED (North, East, Down) frame, defined in a plane tangent to the surface of the Earth at a fixed point in the area of operation of the vehicle.

The position of the origin of $\{\mathcal{B}\}$ in $\{\mathcal{I}\}$ is denoted by

$$\boldsymbol{p} = [x,\ y]^T \tag{1}$$

The velocities of the vehicle with respect to the fluid are expressed in $\{\mathcal{B}\}$ by the surge speed u (linear velocity along x_B), the sway speed v (linear velocity along y_B), and the yaw rate r (angular velocity about z_B). The yaw angle ψ is the angle between the x_I axis and the velocity vector of the vehicle with respect to $\{\mathcal{I}\}$, positive in the clockwise direction.

B. AUV model

We consider the kinematics of an AUV, assuming that an independent depth and pitch controller restrains the motion to a horizontal plane. The linear and angular velocity in $\{\mathcal{I}\}$ are obtained from their counterparts in $\{\mathcal{B}\}$ by

$$\begin{aligned} \dot{\boldsymbol{p}} &= R(\psi)\boldsymbol{v} + \boldsymbol{V_c} \\ \dot{\psi} &= r \end{aligned} \tag{2}$$

The velocity of the vehicle with respect to the water is denoted by $\boldsymbol{v} = [u,\, v]^T$, with u (surge speed) and v (sway speed) expressing this velocity along the x_B and y_B axes respectively; r denotes the yaw rate of the vehicle. The velocity of the current in $\{\mathcal{I}\}$ is denoted by $\boldsymbol{V_c}$. The rotation matrix is

$$R(\psi) = \begin{bmatrix} \cos(\psi) & -\sin(\psi) \\ \sin(\psi) & \cos(\psi) \end{bmatrix} \tag{3}$$

Under simplifying assumptions of low-speed and vehicle symmetry, and neglecting the motions in heave, roll and pitch, the dynamics of the vehicle are given in matrix form [13] by

$$M\dot{\boldsymbol{\nu}} + C(\boldsymbol{\nu})\boldsymbol{\nu} + D(\boldsymbol{\nu})\boldsymbol{\nu} = \boldsymbol{\tau} \tag{4}$$

with

$$M = \begin{bmatrix} m_u & 0 & 0 \\ 0 & m_v & 0 \\ 0 & 0 & m_r \end{bmatrix} > 0$$

$$C(\boldsymbol{v}) = \begin{bmatrix} 0 & 0 & -m_v v \\ 0 & 0 & m_u u \\ m_v v & -m_u u & 0 \end{bmatrix} \text{ (skew-symmetric)}$$

$$D(\boldsymbol{v}) = \begin{bmatrix} d_u & 0 & 0 \\ 0 & d_v & 0 \\ 0 & 0 & d_r \end{bmatrix} > 0$$

$$\begin{aligned} m_u &= m - X_{\dot{u}} \quad & m_r &= I_z - N_{\dot{r}} \quad & d_u &= -X_u - X_{|u|u}\,|u| \\ m_v &= m - Y_{\dot{v}} \quad & m_{uv} &= m_u - m_v \quad & d_v &= -X_v - X_{|v|v}\,|v| \\ & & & & d_r &= -N_r - N_{|r|r}\,|r| \end{aligned}$$

In this paper, we consider only the case where the vehicle is not actuated along y_B, i.e. $\tau_v = 0$.

III. Trajectory-Tracking

A. Problem definition

Trajectory-tracking consists of forcing a vehicle to reach and follow a time-parametrized reference trajectory, by making the vehicle approach a *virtual target* that moves along the reference trajectory with an associated timing law. We denote by $\boldsymbol{p}(t)$ the position of the vehicle and by $\boldsymbol{p}_d(t)$ the desired position, or position of the virtual target, at time t. We give a definition of this problem adapted for the 2D case from [2].

Problem 1 (Trajectory-tracking)**.** *Consider an underactuated autonomous underwater vehicle with dynamic model (4) and kinematic model (2), with $\tau_v = 0$. Let $\boldsymbol{p}_d(t) : [0, \infty) \to \mathbb{R}^2$ be a given sufficiently smooth time-varying desired trajectory with its time-derivatives bounded. Design a controller such that all the closed-loop signals are bounded and the tracking error $\|\boldsymbol{p}(t) - \boldsymbol{p}_d(t)\|$ converges to a neighborhood of the origin that can be made arbitrarily small.*

B. Outer-loop control

We assume a decoupled inner-outer-loop strategy and start by looking at the outer-loop control problem. In this setting, we discard the dynamic model of the vehicle, taking u and r as control variables.

Problem 2 (Outer-loop control)**.** *Consider the kinematic model of the system in (2), with inputs $\boldsymbol{u}_d = (u_d, r_d)$ (commanded surge speed and yaw rate). Assume that these commands are identically satisfied, $\boldsymbol{u}(t) = \boldsymbol{u}_d(t)$. Let $\boldsymbol{p}_d(t) : [0, \infty) \to \mathbb{R}^2$ be a given sufficiently smooth time-varying desired trajectory with its time-derivatives bounded. Design a control law for u and r that produces bounded velocity commands so that the tracking error $\|\boldsymbol{p}(t) - \boldsymbol{p}_d(t)\|$ converges to a neighborhood of the origin that can be made arbitrarily small.*

We start by defining the error variable to be driven to a neighborhood of zero as the position error expressed in $\{\mathcal{B}\}$:

$$\boldsymbol{e} = R^T(\psi)\left(\boldsymbol{p} - \boldsymbol{p}_d\right) \tag{5}$$

where the time-dependence of $\boldsymbol{p}$ and $\boldsymbol{p}_d$ is omitted purely for readability reasons. The time-derivative of $\boldsymbol{e}$ is

$$\begin{aligned}\dot{\boldsymbol{e}} &= R^T(\psi)(\dot{\boldsymbol{p}} - \dot{\boldsymbol{p}}_d) + \dot{R}^T(\psi)(\boldsymbol{p} - \boldsymbol{p}_d) \\ &= R^T(\psi)(\dot{\boldsymbol{p}} - \dot{\boldsymbol{p}}_d) - S(r)R^T(\psi)(\boldsymbol{p} - \boldsymbol{p}_d) \\ &= [u,\ v]^T - R^T(\dot{\boldsymbol{p}}_d - \boldsymbol{V_c}) - S(r)\boldsymbol{e}\end{aligned} \tag{6}$$

where

$$S(r) = \begin{bmatrix} 0 & -r \\ r & 0 \end{bmatrix} \tag{7}$$

For underactuated vehicles, we cannot stabilize $\boldsymbol{e} = 0$ using u and v as control variables, since v cannot be directly controlled. Instead, we resort to rotation to produce lateral motion. By defining a new error variable $\boldsymbol{e}' = \boldsymbol{e} - \boldsymbol{\delta}$ [11], where $\boldsymbol{\delta} = (\delta, 0)$ and $\dot{\delta} = 0$, we obtain new error dynamics:

$$\begin{aligned}\dot{\boldsymbol{e}}' &= \dot{\boldsymbol{e}} - \dot{\boldsymbol{\delta}} \\ &= \begin{bmatrix} u \\ v \end{bmatrix} - R^T(\psi)(\dot{\boldsymbol{p}}_d - \boldsymbol{V_c}) - S(r)(\boldsymbol{e} - \boldsymbol{\delta}) - S(r)\boldsymbol{\delta} \\ &= \underbrace{\begin{bmatrix} 1 & 0 \\ 0 & -\delta \end{bmatrix}}_{\Gamma} \underbrace{\begin{bmatrix} u \\ r \end{bmatrix}}_{\boldsymbol{u}} + \begin{bmatrix} 0 \\ v \end{bmatrix} - R^T(\psi)(\underbrace{\dot{\boldsymbol{p}}_d - \boldsymbol{V_c}}_{\boldsymbol{d}}) - S(r)\boldsymbol{e}'\end{aligned} \tag{8}$$

where the term $\dot{\boldsymbol{p}}_d - \boldsymbol{V_c}$, which includes the velocities of the current and of the target in the inertial frame, is now renamed as a disturbance $\boldsymbol{d}$. In this formulation, if $\boldsymbol{e}'$ is driven to zero, we are driving to the target position a point on the vehicle that lies a distance δ behind the center of mass, along the longitudinal axis.

Assuming that v is not available and that we have incomplete knowledge of $\boldsymbol{d}$, a possible control law is

$$\boldsymbol{u}_d = \Gamma^{-1}\left(R^T(\psi)\hat{\boldsymbol{d}} - K \tanh \frac{\boldsymbol{e}'}{n}\right) \tag{9}$$

with $K = K^T > 0$ and $n > 0$, where $\hat{\boldsymbol{d}}$ is an estimate of $\boldsymbol{d}$ affected by an error $\tilde{\boldsymbol{d}} = \boldsymbol{d} - \hat{\boldsymbol{d}}$. The purpose of the hyperbolic tangent is to saturate the requested velocities due to the position error to a maximum value defined by the gain matrix K. The parameter n adjusts the sensitiveness of the proportional feedback term. We use a definition of the vector-argument hyperbolic tangent that preserves the direction of the vector:

$$\tanh \boldsymbol{x} = \boldsymbol{x}\frac{\tanh \|\boldsymbol{x}\|}{\|\boldsymbol{x}\|} \tag{10}$$

We assume that the speed commands are not identically satisfied, so $\boldsymbol{u}$ may differ from $\boldsymbol{u}_d$. This is because $\boldsymbol{u}_d$ contains requested velocities to be fed to an inner-loop, and it is reasonable to assume that they are not tracked exactly. The inner-loop error is denoted by $\tilde{\boldsymbol{u}} = \boldsymbol{u} - \boldsymbol{u}_d$.

Substituting $\boldsymbol{u} = \tilde{\boldsymbol{u}} + \boldsymbol{u}_d$ and (9) in the error dynamics (8), the time-derivative of a Lyapunov function $V = \frac{1}{2}\boldsymbol{e}'^T\boldsymbol{e}'$ along the trajectories of the system is:

$$\begin{aligned}\dot{V} &= -\boldsymbol{e}'^T K \tanh \frac{\boldsymbol{e}'}{n} + \boldsymbol{e}'^T\left(\Gamma\tilde{\boldsymbol{u}} + \begin{bmatrix} 0 \\ v \end{bmatrix} - R^T(\psi)\tilde{\boldsymbol{d}}\right) \\ &= -\boldsymbol{e}'^T K \boldsymbol{e}' \frac{\tanh \|\boldsymbol{e}'/n\|}{\|\boldsymbol{e}'\|} + \boldsymbol{e}'^T\left(\Gamma\tilde{\boldsymbol{u}} + \begin{bmatrix} 0 \\ v \end{bmatrix} - R^T(\psi)\tilde{\boldsymbol{d}}\right) \\ &\leq -(1-\theta)\boldsymbol{e}'^T K \boldsymbol{e}' \frac{\tanh \|\boldsymbol{e}'/n\|}{\|\boldsymbol{e}'\|}\end{aligned} \tag{11}$$

for $0 < \theta < 1$, when

$$\frac{1}{\theta\lambda_{min}(K)} \cdot \left\|\Gamma\tilde{\boldsymbol{u}} + \begin{bmatrix} 0 \\ v \end{bmatrix} - R^T(\psi)\tilde{\boldsymbol{d}}\right\| < 1 \tag{12}$$

$$\|\boldsymbol{e}'\| \geq n \operatorname{arctanh}\left(\frac{1}{\theta\lambda_{min}(K)} \cdot \left\|\Gamma\tilde{\boldsymbol{u}} + \begin{bmatrix} 0 \\ v \end{bmatrix} - R^T(\psi)\tilde{\boldsymbol{d}}\right\|\right) \tag{13}$$

Proposition 1. *Consider the system with state $\boldsymbol{e}'$, with dynamics expressed in (8), in closed-loop with the feedback controller (9). This system is ISS with respect to input $\Gamma\tilde{\boldsymbol{u}} + [0 \quad v]^T - R^T(\psi)\tilde{\boldsymbol{d}}$, with restrictions on the norm of the input.*

C. Closed-loop dynamics

The previous analysis of the outer-loop is useful when the vehicle is already equipped with an inner-loop for tracking the velocity references. Then, based on some knowledge of the characteristics of the inner-loop, the outer-loop can be tuned by adjusting both K and n. However, it does not explicitly take into account the influence of K and n in $\tilde{\boldsymbol{u}}$ and v. To clarify this, we define a representative inner loop control law and look into the dynamics of these two variables. We start the analysis of the inner-loop velocity error using (4) and defining the extended inner-loop error $\tilde{\boldsymbol{\nu}} = \boldsymbol{\nu} - \boldsymbol{\nu}_d$, where

$$\boldsymbol{\nu}_d = \begin{bmatrix} u_d \\ 0 \\ r_d \end{bmatrix} = \underbrace{\begin{bmatrix} 1 & 0 \\ 0 & 0 \\ 0 & 1 \end{bmatrix}}_{I_{32}} \boldsymbol{u}_d \tag{14}$$

The dynamics of $M\tilde{\boldsymbol{\nu}}$ are

$$\begin{aligned}M\dot{\tilde{\boldsymbol{\nu}}} &= -C(\boldsymbol{\nu})\boldsymbol{\nu} - D(\boldsymbol{\nu})\boldsymbol{\nu} + \boldsymbol{\tau} - M\dot{\boldsymbol{\nu}}_d \\ &= -\left[C(\boldsymbol{\nu}) + D(\boldsymbol{\nu})\right]\tilde{\boldsymbol{\nu}} - \left[C(\boldsymbol{\nu}) + D(\boldsymbol{\nu})\right]\boldsymbol{\nu}_d - M\dot{\boldsymbol{\nu}}_d + \boldsymbol{\tau}\end{aligned} \tag{15}$$

A possible inner-loop control law that does not use v or $\dot{\boldsymbol{\nu}}_d$ (because we assume that the only command fed from the outer to the inner-loop is $\boldsymbol{u}_d$) and does not actuate on τ_v is

$$\boldsymbol{\tau} = -\underbrace{\begin{bmatrix} k_u & 0 & 0 \\ 0 & 0 & 0 \\ 0 & 0 & k_r \end{bmatrix}}_{K_d} \tilde{\boldsymbol{\nu}} + D(\boldsymbol{\nu})\boldsymbol{\nu}_d \tag{16}$$

Substituting (16) in (15),

$$M\dot{\tilde{\boldsymbol{\nu}}} = -\left[C(\boldsymbol{\nu}) + D(\boldsymbol{\nu}) + K_d\right]\tilde{\boldsymbol{\nu}} - C(\boldsymbol{\nu})\boldsymbol{\nu}_d - M\dot{\boldsymbol{\nu}}_d \tag{17}$$

where

$$\dot{\boldsymbol{\nu}}_d = I_{32}\Gamma^{-1}\left(-S(r)R^T(\psi)\hat{\boldsymbol{d}} + R^T(\psi)\dot{\hat{\boldsymbol{d}}} - K\frac{d}{dt}\left(\tanh\frac{\boldsymbol{e}'}{n}\right)\right) \tag{18}$$

The derivative of the term with the hyperbolic tangent is

$$\begin{aligned}\frac{d}{dt}\left(\tanh\frac{\boldsymbol{e}'}{n}\right) &= \frac{d}{dt}\left(\frac{\boldsymbol{e}'}{n}\frac{\tanh\|\boldsymbol{e}'/n\|}{\|\boldsymbol{e}'/n\|}\right) \\ &= B(\boldsymbol{e}'/n)\frac{\dot{\boldsymbol{e}}'}{n}\end{aligned} \tag{19}$$

with

$$\dot{\boldsymbol{e}}' = \underbrace{\begin{bmatrix} 1 & 0 & 0 \\ 0 & 1 & -\delta \end{bmatrix}}_{\Gamma_{23}}\tilde{\boldsymbol{\nu}} - K\tanh\frac{\boldsymbol{e}'}{n} - R^T(\psi)\tilde{\boldsymbol{d}} - S(r)\boldsymbol{e}' \tag{20}$$

We do not expand $B(\boldsymbol{e}'/n)$. It is sufficient to state that, for any $\boldsymbol{e}'$, there exist two constants ϵ_1, $\epsilon_2 > 0$ such that

$$\|B(\boldsymbol{e}'/n)\| < \epsilon_1 \tag{21}$$

$$\|B(\boldsymbol{e}'/n)\| \cdot \|\boldsymbol{e}'/n\| < \epsilon_2 \tag{22}$$

We now analyse the stability of the closed-loop system with the tracking error $\boldsymbol{e}'$ and the extended inner-loop error $\tilde{\boldsymbol{\nu}}$ as states, using a Lyapunov function:

$$V = \frac{1}{2}\boldsymbol{e}'^T\boldsymbol{e}' + \frac{1}{2}\tilde{\boldsymbol{\nu}}^T M\tilde{\boldsymbol{\nu}} \tag{23}$$

Differentiating each term and grouping quadratic and linear terms in each of the states, and terms involving the product of $\boldsymbol{e}'$ and $\tilde{\boldsymbol{\nu}}$, we obtain

$$\begin{aligned}\dot{V} &= \boldsymbol{e}'^T\dot{\boldsymbol{e}}' + \tilde{\boldsymbol{\nu}}^T M\dot{\tilde{\boldsymbol{\nu}}} \\ &= -\boldsymbol{e}'^T K\boldsymbol{e}'\frac{\tanh\|\boldsymbol{e}'/n\|}{\|\boldsymbol{e}'\|} + \boldsymbol{e}'^T\boldsymbol{b} + \tilde{\boldsymbol{\nu}}^T\boldsymbol{a} + \tilde{\boldsymbol{\nu}}^T A\boldsymbol{e}' \\ &\quad - \tilde{\boldsymbol{\nu}}^T\left(D(\boldsymbol{\nu}) + K_d - MI_{32}\Gamma^{-1}K\frac{B(\boldsymbol{e}'/n)}{n}\Gamma_{23}\right)\tilde{\boldsymbol{\nu}}\end{aligned} \tag{24}$$

where

$$\begin{aligned}\boldsymbol{a} = -C(\boldsymbol{\nu})\boldsymbol{\nu}_d - MI_{32}\Gamma^{-1}\Big(&-S(r)R^T(\psi)\hat{\boldsymbol{d}} + R^T(\psi)\dot{\hat{\boldsymbol{d}}} \\ &+K\frac{B(\boldsymbol{e}'/n)}{n}\left(K\tanh\frac{\boldsymbol{e}'}{n} + R^T(\psi)\tilde{\boldsymbol{d}} + S(r)\boldsymbol{e}'\right)\Big)\end{aligned} \tag{25}$$

$$\boldsymbol{b} = -R^T(\psi)\tilde{\boldsymbol{d}} \tag{26}$$

$$A = \Gamma_{23}^T \tag{27}$$

Note that $\|\boldsymbol{b}\| = \|\tilde{\boldsymbol{d}}\|$. Taking norms and applying Young's inequality to the term $\tilde{\boldsymbol{\nu}}^T A\boldsymbol{e}'$, we obtain:

$$\begin{aligned}\dot{V} &\leq -\lambda_{min}(K)\|\boldsymbol{e}'\|\tanh\|\boldsymbol{e}'/n\| + \|\boldsymbol{e}\|\|\tilde{\boldsymbol{d}}\| + \frac{\epsilon\|\boldsymbol{e}'\|^2}{2} \\ &\quad - \tilde{\boldsymbol{\nu}}^T K_v\tilde{\boldsymbol{\nu}} + \|\tilde{\boldsymbol{\nu}}\|\|\boldsymbol{a}\| \\ &= \dot{V}_{\boldsymbol{e}'} + \dot{V}_{\tilde{\boldsymbol{\nu}}}\end{aligned} \tag{28}$$

for some $\epsilon > 0$, with

$$K_v = D(\boldsymbol{\nu}) + K_d - MI_{32}\Gamma^{-1}K\frac{B(\boldsymbol{e}'/n)}{n}\Gamma_{23} - \frac{\left\|\Gamma_{23}^T\right\|^2}{2\epsilon} \tag{29}$$

If $K, K_v > 0$ and there exists some $0 < \theta_{\boldsymbol{e}'} < 1$ such that

$$\frac{\|\tilde{\boldsymbol{d}}\| + \frac{\epsilon\|\boldsymbol{e}'\|}{2}}{\theta_{\boldsymbol{e}'}\lambda_{min}(K)} < 1 \tag{30}$$

then $\dot{V}_{\boldsymbol{e}'} < 0$ when

$$\|\boldsymbol{e}'\| > n\,\mathrm{arctanh}\,\frac{\|\tilde{\boldsymbol{d}}\| + \frac{\epsilon\|\boldsymbol{e}'\|}{2}}{\theta_{\boldsymbol{e}'}\lambda_{min}(K)} \tag{31}$$

For a fixed K and $\|\tilde{\boldsymbol{d}}\|$, (30) cannot be satisfied for arbitrarily large $\boldsymbol{e}'$ because of the term $\frac{\epsilon\|\boldsymbol{e}'\|}{2}$. Indeed, this condition implies a restriction on the norm of the initial state $\boldsymbol{e}'(0)$. To relax this restriction, in the analysis ϵ can be chosen small enough, at the expense of more conservative conditions for $\tilde{\boldsymbol{\nu}}$.

We now look at $\dot{V}_{\tilde{\boldsymbol{\nu}}}$. Two important aspects should be noted, regarding the structure of the D and C matrices:

- The entries of the D matrix contain only terms that are constant or linear in $\boldsymbol{\nu}$. Hence, because $\boldsymbol{\nu} = \tilde{\boldsymbol{\nu}} + \boldsymbol{\nu}_d$, it can be decomposed by $D(\boldsymbol{\nu}) = D'(\tilde{\boldsymbol{\nu}}) + D(\boldsymbol{\nu}_d)$ where D' is a modified drag matrix obtained by removing the constant terms.
- Similarly, the entries of the C matrix contain only terms that are linear in $\boldsymbol{\nu}$, so $C(\boldsymbol{\nu}) = C(\tilde{\boldsymbol{\nu}}) + C(\boldsymbol{\nu}_d)$.

We now state without proof two propositions concerning $\dot{V}_{\tilde{\boldsymbol{\nu}}}$ that will be instrumental in proving the stability result.

Proposition 2. *The term $\tilde{\boldsymbol{\nu}}^T D(\boldsymbol{\nu})\tilde{\boldsymbol{\nu}}$ is lower-bounded by a term proportional to $\|\tilde{\boldsymbol{\nu}}\|^3$ as $\|\tilde{\boldsymbol{\nu}}\| \to \infty$.*

Proposition 3. *All the terms in $\tilde{\boldsymbol{\nu}}^T K_v\tilde{\boldsymbol{\nu}}$, other than the drag-related ones, are upper-bounded by a term proportional to $\|\tilde{\boldsymbol{\nu}}\|^2$ as $\|\tilde{\boldsymbol{\nu}}\| \to \infty$. The same happens with $\|\tilde{\boldsymbol{\nu}}\|\,\|\boldsymbol{a}\|$.*

These observations allow us to conclude that there must exist some sufficiently large $\tilde{\boldsymbol{\nu}}$ such that $\tilde{\boldsymbol{\nu}}^T K_v\tilde{\boldsymbol{\nu}}$ is greater than $\tilde{\boldsymbol{\nu}}^T\boldsymbol{a}$. Hence, $\dot{V}_{\tilde{\boldsymbol{\nu}}} < 0$ for sufficiently large $\tilde{\boldsymbol{\nu}}$.

Proposition 4. *Consider the system with states $\boldsymbol{e}'$ and $\tilde{\boldsymbol{\nu}}$, whose dynamics are expressed in (8) and (15), in closed-loop with the feedback control laws (9) and (16). Consider as inputs 1) the disturbance estimation error $\tilde{\boldsymbol{d}}$, which contains the estimation error regarding the current and the velocity of the target, 2) the disturbance estimate $\hat{\boldsymbol{d}}$, and 3) the time-derivative of the disturbance estimate $\dot{\hat{\boldsymbol{d}}}$. For appropriately chosen controller parameters K, n, K_d and δ, the system is bounded-input bounded-state (BIBS) with restrictions on $\|\tilde{\boldsymbol{d}}\|$.*

Proof: Consider the Lyapunov function V defined in (23) and its time-derivative (24). Note that if $\|\tilde{\boldsymbol{d}}\|$ and ϵ are small enough for condition (30) to be verified, then for sufficiently large $\boldsymbol{e}'$ satisfying (31), the derivative of the terms of the Lyapunov function concerning $\boldsymbol{e}'$ is negative definite:

$$\dot{V}_{\boldsymbol{e}'} \leq -(1 - \theta_{\boldsymbol{e}'})\boldsymbol{e}'^T K\boldsymbol{e}'\frac{\tanh\|\boldsymbol{e}'/n\|}{\|\boldsymbol{e}'\|} < 0 \tag{32}$$

Consider now the terms of the derivative of the Lyapunov function concerning $\tilde{\boldsymbol{\nu}}$:

$$\dot{V}_{\tilde{\boldsymbol{\nu}}} \leq -(1 - \theta_{\tilde{\boldsymbol{\nu}}})\tilde{\boldsymbol{\nu}}^T K_v\tilde{\boldsymbol{\nu}} - \theta_{\tilde{\boldsymbol{\nu}}}\tilde{\boldsymbol{\nu}}^T K_v\tilde{\boldsymbol{\nu}} + \|\tilde{\boldsymbol{\nu}}\|\,\|\boldsymbol{a}\| \tag{33}$$

Given Propositions 2 and 3, for large enough $\|\tilde{\boldsymbol{\nu}}\|$,

$$\dot{V}_{\tilde{\boldsymbol{\nu}}} \leq -(1-\theta_{\tilde{\boldsymbol{\nu}}})\tilde{\boldsymbol{\nu}}^T K_v \tilde{\boldsymbol{\nu}} < 0 \tag{34}$$

Since $\dot{V} \leq \dot{V}_{\boldsymbol{e}'} + \dot{V}_{\tilde{\boldsymbol{\nu}}}$, as long as condition (30) is satisfied, the local version of Theorem 4.9 from [14] can be applied to conclude the BIBS property. ■

The result is derived for the model structure given before, without considering any numerical values. Consequently, the result is general enough to apply to a wide range of vehicles.

Remark 1. In practice, the tracking error converges to zero even when the virtual target moves with a non-null, known constant velocity vector. This is not captured by the result stated above because the Lyapunov function used is not always strictly decreasing along trajectories of the system. Had the closed-loop system been analysed using different Lyapunov functions, or theory of interconnected systems, we might have been able to prove convergence at the expense of a much more cumbersome analysis. This convergence, however, is still proved by the outer-loop analysis in Section III-B, if we ignore the dynamics of the vehicle by setting $\tilde{\boldsymbol{u}} = 0$ and $v = 0$.

D. Application to Formation Control

The trajectory-tracking algorithm presented above can be fed signals from a new block, called a path generator, responsible for generating a virtual target in such a way that the formation objectives are met. This virtual target would then be tracked by the trajectory-tracking algorithm. If this virtual target does not depend on the motion of the vehicle, a feedback connection between the path-generator and the trajectory-tracking controller is avoided, which greatly simplifies the stability analysis. Figure 2 illustrates the structure of the entire system, including this new path generator block.

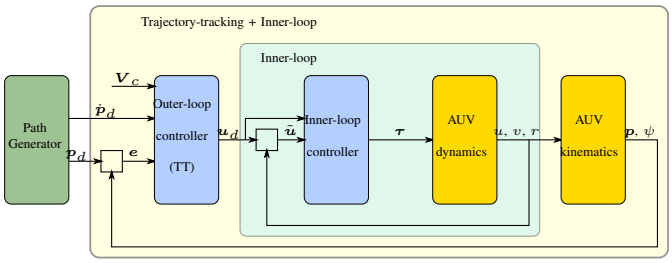

Figure 2: Block diagram of the complete system, including the path generator.

IV. Formation Control

We now look at the problems of keeping formations based on 1) relative position measurements or 2) range-only measurements. Only the case where the formation has a leader-follower topology is considered.

A. Formation control with relative position measurements

We start by considering the formation control problem that arises in the context of the MORPH upper segment: driving GCV and LSV (followers) to appropriate positions relative to SSV (leader), using *relative position measurements* obtained from a USBL (that can be placed in any vehicle), without any direct communication between the SSV and LSV. Several possible formation strategies could be used, but due to its properties concerning the effect of currents or sideslip and the typical mission geometries (lawnmower-like shapes), we use a *non-rigid formation based on the previous path of the leader*. The formation is specified by two parameters, δ_x and δ_y. The first parameter, δ_x, defines the desired distance between the leader and the follower *along the path of the leader*. After moving this distance backwards along the path, the position of the virtual target is then obtained by moving a distance of δ_y perpendicular to the path of the leader. This is illustrated in Figure 3.

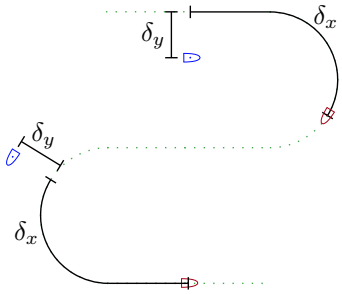

Figure 3: Desired position of a follower vehicle based on the trajectory described by the leader vehicle.

In order to use a path-generator that computes the position of a virtual target according to this formation strategy, a follower vehicle should have information regarding the previous path of the leader. To minimize the information exchanged between vehicles and adopt an approach that scales easily with the number of followers, some assumptions are made regarding the path of the leader:

1) It contains only alternating *straight-line and constant-curvature segments*;
2) The virtual target of the follower is always either in the same segment as the leader or in the previous one.

Given these two assumptions, *the leader only needs to broadcast three parameters*: its total velocity V_L in $\{\mathcal{I}\}$, course angle χ_L and its derivative $\dot{\chi}_L$. The path can be generated in such a way that it only depends on the *present values* of V_L, χ_L and $\dot{\chi}_L$, so integration of past data is avoided. We can now define the problem to be solved by the path-generator block in a clear manner.

Problem 3 (Path-generation with relative position measurements)**.** *Consider a leader vehicle performing a mission consisting of a continuous concatenation of path segments. The path segments alternate between straight lines and constant-radius turns. Consider now a virtual target to be tracked by the follower vehicle, assumed to be in the same or previous path segment as the leader vehicle at all times. Assume that the total velocity V_L, course angle χ_L and course angle rate $\dot{\chi}_L$ of the leader are continuously broadcast.*

Derive a path-generation strategy that computes the position and velocity of the virtual target to be tracked by the follower vehicle, such that the follower vehicle moves in a formation with the leader according to the formation strategy presented above. The position and velocity of the virtual target should be provided by the path-generator as an error vector in the follower's body-frame $\{\mathcal{B}\}$ and an inertial velocity in $\{\mathcal{I}\}$, i.e. the parameters $\boldsymbol{e}$ and $\dot{\boldsymbol{p}}_d$ as defined in Section III-B.

To address this problem, we first note that the three parameters broadcast by the leader do not contain information

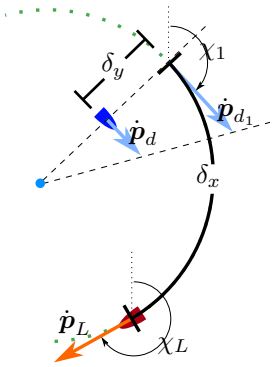

Figure 4: Position and velocity of the point to be tracked (in blue), based on the motion of the leader (in red).

about its position. For now we assume that the position of the leader with respect to a follower is available via USBL measurements.

We now derive the equations to obtain $\boldsymbol{e}$ and $\dot{\boldsymbol{p}}_d$, assuming that the leader and the virtual target lie in the same segment of the path. This assumption is lifted later. Figure 4 illustrates the process and contains the necessary vectors and angles for easier understanding of the derivation.

The body-frame error vector as defined in Section III-B is

$$\boldsymbol{e} = R^T(\psi)\,(\boldsymbol{p} - \boldsymbol{p}_d) \tag{35}$$

To compute $\boldsymbol{e}$, we first need to determine $\boldsymbol{p}_d$. To this end, we first integrate the leader's velocity vector backwards over a path with course angle rate $\dot{\chi}$, over a distance of δ_x:

$$\boldsymbol{p}_{d_1} = \boldsymbol{p}_L - \int_0^{\frac{\delta_x}{V_L}} R(-\dot{\chi}_L t) \overbrace{\left(R(\chi_L)\begin{bmatrix}V_L\\0\end{bmatrix}\right)}^{\text{leader's velocity vector}} dt \tag{36}$$

We obtain the final equation for $\boldsymbol{p}_d$ by adding a vector of length δ_y in a direction perpendicular to the integrand in (36) with $t = \delta_x/V_L$, yielding

$$\boldsymbol{p}_d = \boldsymbol{p}_L - \int_0^{\frac{\delta_x}{V_L}} R(\chi_L - \dot{\chi}_L t)\begin{bmatrix}V_L\\0\end{bmatrix} dt + R(\chi_L - \dot{\chi}_L \frac{\delta_x}{V_L})\begin{bmatrix}0\\\delta_y\end{bmatrix} \tag{37}$$

which now allows us to compute $\boldsymbol{e}$. The velocity of the virtual target $\dot{\boldsymbol{p}}_d$ is given by

$$\dot{\boldsymbol{p}}_d = R(\chi_L - \dot{\chi}_L \frac{\delta_x}{V_L})\begin{bmatrix}V_L\\0\end{bmatrix} + R(\chi_L - \dot{\chi}_L \frac{\delta_x}{V_L})S(\dot{\chi}_L)\begin{bmatrix}0\\\delta_y\end{bmatrix} \tag{38}$$

where we assumed that the formation parameters are constant, $\dot{\delta}_x = \dot{\delta}_y = 0$, and that the radius of curvature of the leader's path is constant, $\frac{d}{dt}\frac{V_L}{\dot{\chi}_L} = 0$. These expressions are also valid for $\dot{\chi}_L = 0$.

To lift the assumption that the leader and virtual target lie in the same segment of the path, we introduce an algorithm that handles the cases when this is not true.

1) Generate $\boldsymbol{e}$ and $\dot{\boldsymbol{p}}_d$ using (37) and (38).
2) If the generated position of the virtual target deviates more than a threshold ϵ from its current position, then there is a discontinuity in the generated path, so the leader and the virtual target are not in the same segment - we proceed to step 3. Otherwise, the algorithm returns the values obtained from step 1.
3) If the present value of $\dot{\chi}_L$ is non-zero, the leader is in a turn and the virtual target is in a straight segment. We compute $\boldsymbol{e}$ by integrating backwards along the path of the leader *in a turn until a certain point*, and then in a straight line. We use (37) with two modifications:
   - The integral term in (37) is computed with the present value of $\dot{\chi}_L$ until the direction of the path being generated matches the direction in which the virtual target is moving. The remainder of the integral is computed with $\dot{\chi}_L = 0$.
   - The last term in (37) is computed with $\chi_L - \dot{\chi}_L \frac{\delta_x}{V_L}$ replaced by the course angle of the virtual target.

   To compute $\dot{\boldsymbol{p}}_d$, we use (38) with two modifications:
   - In the first term, $\chi_L - \dot{\chi}_L \frac{\delta_x}{V_L}$ is replaced by the course angle of the virtual target.
   - The last term vanishes.
4) If the present value of $\dot{\chi}_L$ is zero, then the leader is in a straight line and the virtual target is in a turn. We integrate backwards along the path of the leader *in a straight line until a certain point*, and then in a turn. A procedure similar to step 3 is used.

Besides $\boldsymbol{e}$ and $\dot{\boldsymbol{p}}_d$, the trajectory-tracking controller also needs an estimate of velocity of the current measured and expressed in $\{\mathcal{I}\}$, $\boldsymbol{V_c}$. We now derive an estimator for the current that can be placed in a cascade interconnection with the controller.

We know that each follower must have access to its position relative to the leader. For simplicity, we consider that this relative position is available in $\{\mathcal{I}\}$. If it is only available in $\{\mathcal{B}\}$, it can be transformed to $\{\mathcal{I}\}$ through left-multiplication by $R(\psi)$. We denote this relative position in $\{\mathcal{I}\}$ by

$$\boldsymbol{e}_U = \boldsymbol{p} - \boldsymbol{p}_L \tag{39}$$

where the subscript U is used to clarify that this estimation concerns the upper segment vehicles. The dynamics of $\boldsymbol{e}_U$ are

$$\begin{aligned}\dot{\boldsymbol{e}}_U &= \dot{\boldsymbol{p}} - \dot{\boldsymbol{p}}_L \\ &= R(\psi)\begin{bmatrix}u\\0\end{bmatrix} - \dot{\boldsymbol{p}}_L + \boldsymbol{V}_c + R(\psi)\begin{bmatrix}0\\v\end{bmatrix}\end{aligned} \tag{40}$$

with

$$\dot{\boldsymbol{p}}_L = R(\chi_L)\begin{bmatrix}V_L\\0\end{bmatrix} \tag{41}$$

The first two terms in (40) are inputs to the estimator:

$$\boldsymbol{z}_U = R(\psi)\begin{bmatrix}u\\0\end{bmatrix} - \dot{\boldsymbol{p}}_L \tag{42}$$

Consider now a system with $\boldsymbol{x}_U = [\boldsymbol{e}_L \quad \boldsymbol{V}_c]^T$ as states, where $\dot{\boldsymbol{V}}_c = 0$:

$$\dot{\boldsymbol{x}}_U = \underbrace{\begin{bmatrix}0 & I_2\\0 & 0\end{bmatrix}}_{A}\boldsymbol{x}_U + \underbrace{\begin{bmatrix}I_2\\0\end{bmatrix}}_{B}\boldsymbol{z}_U + \begin{bmatrix}R(\psi)\\0\end{bmatrix}\begin{bmatrix}0\\v\end{bmatrix} \tag{43}$$

If we define an observer with identical dynamics (except for the unknown sway) and include a feedback on $\boldsymbol{e}_U$,

$$\dot{\hat{\boldsymbol{x}}}_U = A\hat{\boldsymbol{x}}_U + B\boldsymbol{z}_U + K_o\underbrace{\begin{bmatrix}I_2 & 0\end{bmatrix}}_{C}(\boldsymbol{x}_U - \hat{\boldsymbol{x}}_U) \tag{44}$$

then the dynamics of the estimation error $\tilde{\boldsymbol{x}}_U = \boldsymbol{x}_U - \hat{\boldsymbol{x}}_U$ are

$$\dot{\tilde{\boldsymbol{x}}}_U = (A - K_oC)\tilde{\boldsymbol{x}}_U + \underbrace{\begin{bmatrix}R(\psi)\\0\end{bmatrix}\begin{bmatrix}0\\v\end{bmatrix}}_{\boldsymbol{b}} \tag{45}$$

where the last term was renamed as a disturbance $\boldsymbol{b}$. The eigenvalues of $L = A - K_o C$ can be chosen arbitrarily by appropriate choice of K_o, because the pair (A, C) is observable. If all the eigenvalues are chosen with negative real part, L is Hurwitz. Then, for all $Q = Q^T > 0$, there is a unique solution $P = P^T > 0$ to the Lyapunov equation:

$$L^T P + PL + Q = 0 \tag{46}$$

Using a Lyapunov function $V = \tilde{\boldsymbol{x}}_U^T P \tilde{\boldsymbol{x}}_U$:

$$\begin{aligned} \dot{V} &= (L\tilde{\boldsymbol{x}}_U + \boldsymbol{b})^T P \tilde{\boldsymbol{x}}_U + \tilde{\boldsymbol{x}}_U^T P (L\tilde{\boldsymbol{x}}_U + \boldsymbol{b}) \\ &= -\|\tilde{\boldsymbol{x}}_U\|^2 + 2\tilde{\boldsymbol{x}}_U^T P \boldsymbol{b} \end{aligned} \tag{47}$$

The estimator is ISS with respect to $\boldsymbol{b}$. The observer dynamics should now be introduced in the closed-loop analysis, but this would make the calculations significantly more complex. As such, we make the simplifying assumption that no considerable interactions exist between the two loops; this could be a consequence, for example, of ignoring the dynamics of the vehicle and considering only the kinematics.

Proposition 5. *Using the path-generator described above, the inner and outer-loop controllers described and analysed in the previous section, and the estimator described in the present section, the formation error of the upper segment vehicles (position error with respect to where a vehicle should be to satisfy the formation constraints) remains bounded.*

Also, recall the remark from the closed-loop analysis in Section III-C: although the result obtained does not prove asymptotic stability when the target moves with a constant known velocity vector, this is observed in practice. It can also be concluded from the outer-loop analysis in Section III-B if the dynamics of the vehicle are ignored by setting $\tilde{\boldsymbol{u}} = 0$ and $v = 0$. Under these assumptions, if we assume that the velocity vector of the target is not known but estimated using the observer presented above, *the tracking error converges to zero when the acceleration of the virtual target $\ddot{\boldsymbol{p}}_d$ is zero.*

The strategies derived above can be used in the MORPH upper segment by considering that GCV and LSV both follow the SSV and run their own path-generator, controller and estimator. Both followers should have access to their position relative to the leader and the necessary leader path parameters. However, only one USBL is available and the SSV cannot communicate directly with the LSV. A solution that allows both followers to know their positions relative to the leader and the leader path parameters is to *use the GCV to relay information to the LSV*. This can be accomplished by placing the USBL on the GCV and equipping the SSV and LSV with transponders. Figure 6 illustrates a possible information flow between the three vehicles in the MORPH upper segment, along with the lower segment which is discussed next.

B. Formation control with range-only measurements

The problem of formation control with range-only measurements arises when a follower vehicle does not have access to its position relative to the leader vehicle, but only the *range* between them. In MORPH, the camera vehicles C1V and C2V (followers) should use this kind of formation control.

A natural first step when approaching this problem is to determine how a follower can obtain information concerning its position. Since the lower segment followers have access to range measurements to two leaders (GCV and LSV), if the distance d between the two leaders is known, a follower can infer its position in a *mobile frame* $\{\mathcal{M}\}$ *apart from a reflection ambiguity*. This frame is oriented with the line between the two upper segment vehicles, with the origin at the midpoint of that line. This is illustrated in Figure 5, with the two leader vehicles shown in green and red, and the two possible positions of the follower vehicle in blue. The ranges between the follower and the leaders are denoted by d_1 and d_2. A simple workaround to disambiguate the position of the follower is to make one of the leaders - the GCV, which carries a USBL transceiver - broadcast a bit that determines whether the follower lies on the semi-plane with positive or negative y_M. Obviously, with more than one follower, one bit per follower would have to be broadcast, but this would still be a very small amount of data. The distance d between the leaders is available to C1V and C2V as a consequence of the communication architecture currently implemented in MORPH. Following simple geometrical calculations, the position of a follower in $\{\mathcal{M}\}$, denoted by ${}^M\boldsymbol{p} = ({}^M p_x, {}^M p_y)$, is given by

$${}^M p_x = -\frac{d_1^2 - d_2^2}{2d} \tag{48}$$

$${}^M p_y = \pm\sqrt{d_1^2 - \left({}^M p_x - \frac{d}{2}\right)^2} \tag{49}$$

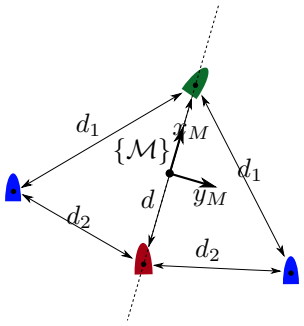

Figure 5: Ambiguity when determining the position of a follower in $\{\mathcal{M}\}$ based on the ranges between the follower and two upper segment vehicles.

We now assume that, according to previous discussion, GCV broadcasts a disambiguating bit and hence each follower knows its position in the mobile frame, ${}^M\boldsymbol{p}$, without the ambiguity in ${}^M p_y$.

Problem 4 (Path-generation with range-only measurements)**.** *Consider two leader vehicles moving along arbitrary trajectories. Consider now a follower vehicle that has knowledge of its position ${}^M\boldsymbol{p}$ in a mobile frame $\{\mathcal{M}\}$ as defined above.*

Derive a path-generation strategy that computes the position and velocity of the virtual target to be tracked by the follower vehicle, such that the follower vehicle is driven to a constant position in $\{\mathcal{M}\}$. This position and velocity of the virtual target should be provided by the path-generator as an error vector in $\{\mathcal{B}\}$ and an inertial velocity in $\{\mathcal{I}\}$, i.e. the parameters $\boldsymbol{e}$ and $\dot{\boldsymbol{p}}_d$ as defined in Section III-B.

We introduce some notation to tackle this problem: $\boldsymbol{p}_M$ is the position of the origin of $\{\mathcal{M}\}$, expressed in $\{\mathcal{I}\}$; ψ_M is the angle between the x axis of $\{\mathcal{I}\}$ and the x axis of $\{\mathcal{M}\}$; ${}^M\boldsymbol{p}$ is the position of the follower vehicle, expressed in $\{\mathcal{M}\}$; is the position of the virtual target, expressed in $\{\mathcal{M}\}$, and assumed to be constant. The assumption that the two leaders move

along arbitrary trajectories is equivalent to assuming that $\{\mathcal{M}\}$ moves arbitrarily. We introduce some parameters concerning this motion: $\dot{\boldsymbol{p}}_M$ is the velocity of the origin of $\{\mathcal{M}\}$ with respect to $\{\mathcal{I}\}$, expressed in $\{\mathcal{I}\}$; $\dot{\psi}_M$ is the angular rate of $\{\mathcal{M}\}$ about its origin.

We can now write the positions of the virtual target and of the follower vehicle in $\{\mathcal{I}\}$:

$$\boldsymbol{p}_d = \boldsymbol{p}_M + R(\psi_M)\,{}^M\boldsymbol{p}_d \tag{50}$$

$$\boldsymbol{p} = \boldsymbol{p}_M + R(\psi_M)\,{}^M\boldsymbol{p} \tag{51}$$

The body-frame position error can be written as:

$$\boldsymbol{e} = R^T(\psi)R(\psi_M)\left({}^M\boldsymbol{p} - {}^M\boldsymbol{p}_d\right) \tag{52}$$

We differentiate (50) to determine $\dot{\boldsymbol{p}}_d$:

$$\begin{aligned}\dot{\boldsymbol{p}}_d &= \dot{\boldsymbol{p}}_M + \dot{R}(\psi_M)\,{}^M\boldsymbol{p}_d + R(\psi_M)\,{}^M\dot{\boldsymbol{p}}_d \\ &= \dot{\boldsymbol{p}}_M + R(\psi_M)S(\dot{\psi}_M)\,{}^M\boldsymbol{p}_d\end{aligned} \tag{53}$$

It is now visible that three new parameters are needed besides those already discussed: ψ_M, $\dot{\psi}_M$ and $\dot{\boldsymbol{p}}_M$. The orientation of the mobile frame ψ_M be computed by the GCV, since it has access to its position relative to the LSV; it is then broadcast to the lower-segment vehicles. However, $\dot{\psi}_M$ and $\dot{\boldsymbol{p}}_M$ cannot be computed by any vehicle without introducing extra communications between upper segment vehicles. The lower segment vehicles will not have complete access to the velocity of their virtual targets - they will have to rely on an estimate.

Following a strategy analogous to the observer for the upper segment, but considering $\boldsymbol{d} = \dot{\boldsymbol{p}}_L - \boldsymbol{V}_c$ as the variable to be estimated and using $\boldsymbol{p} - \boldsymbol{p}_d$, we obtain an observer with estimation error dynamics given by

$$\dot{\tilde{\boldsymbol{x}}}_L = (A - K_o C)\tilde{\boldsymbol{x}}_L + \begin{bmatrix} R(\psi) & 0 \\ 0 & I_2 \end{bmatrix} \left[\begin{array}{c} 0 \\ v \\ \hline \ddot{\boldsymbol{p}}_d \end{array}\right] \tag{54}$$

The remarks on observability and ISS stated for the upper segment still apply, the difference being that $\boldsymbol{b}$ now includes the extra term $\ddot{\boldsymbol{p}}_d$. Given this, we can recover the result on boundedness of the formation error for the vehicles in the upper segment, and adapt it to the lower segment by enforcing an additional condition on $\ddot{\boldsymbol{p}}_d$.

Proposition 6. *Assume that the acceleration of the virtual target is small enough for the error of the estimator described above to converge to a small neighborhood of zero. Under the same assumptions established in Proposition 5, using the path-generator described in this section, the inner and outer-loop controllers described and analysed in the previous section, and the estimator described in the present section, the formation error of the lower segment vehicles (position error with respect to where a vehicle should be to satisfy the formation constraints) remains bounded.*

The path-generator and estimator described above for the lower segment vehicles can be directly used in the lower segment of MORPH by making the camera vehicles C1V and C2V followers and GCV and LSV leaders. Each camera vehicle has a defined desired position in the mobile frame $\{\mathcal{M}\}$. The desired positions for C1V and C2V should be separated by a reasonable distance to avoid collisions.

Two parameters need to be broadcast by the GCV to the lower segment to enable the camera vehicles to keep the formation: ψ_M and one disambiguation bit per camera vehicle. Figure 6 shows an information flow diagram for the lower segment, and includes also the upper segment.

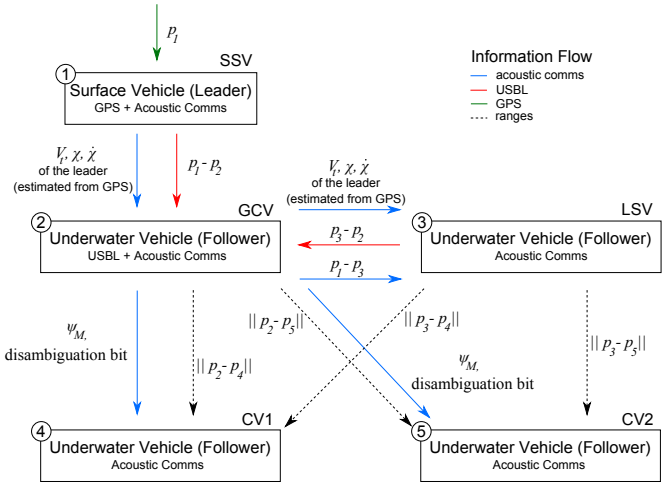

Figure 6: Information flow in MORPH.

V. Implementation

We now describe modifications introduced in the proposed control and estimation strategies, to allow implementation of the upper segment formation control in MEDUSA vehicles.

A. Trajectory-tracking controller

For the MEDUSA vehicles, a PID inner-loop controller was already available, accepting commands in u and ψ. The outer-loop is adapted so that it provides surge speed and heading requests (u_d and ψ_d) instead of surge speed and yaw rate. We left-multiply the outer-loop controller in (9) by $R(\psi)\,\Gamma$ to obtain the desired velocity vector with respect to the water, expressed in $\{\mathcal{I}\}$. Multiplication by Γ recovers the desired velocity vector with respect to the water, in $\{\mathcal{B}\}$, before the redefinition of the error variable (from $\boldsymbol{e}$ to $\boldsymbol{e}'$); multiplication by $R(\psi)$ then rotates this vector to $\{\mathcal{I}\}$:

$$\boldsymbol{V}_d = \hat{\boldsymbol{d}} - R(\psi)K\tanh\frac{\boldsymbol{e}}{n} \tag{55}$$

We define the commanded surge speed and heading as the norm and angle of $\boldsymbol{V}_d$, defined in such a way that

$$R(\angle\boldsymbol{V}_d)\begin{bmatrix}\|\boldsymbol{V}_d\| \\ 0\end{bmatrix} = \boldsymbol{V}_d \tag{56}$$

In MORPH, the nominal speeds of the vehicles are low and the radii of curvature are considerable. Then, we can assume that the sway speed and inner-loop error are negligible, so $v \approx 0$, $\psi \approx \psi_d$, $u \approx u_d$. In this situation, the tracking error dynamics are identical to those obtained in Section III-B, so the outer-loop ISS result from Proposition 1 still applies.

This controller was run in discrete-time, at 5 Hz.

B. Filtering and estimation

We now describe the necessary filtering architecture implemented in the upper segment vehicles, consisting of two Kalman filters developed in collaboration with Mohammadreza Bayat. An additional filter running in the leader vehicle to estimate V_L, χ_L and $\dot{\chi}_L$ from GPS position measurements was implemented but not used at the sea trials, so it is not shown here; the nominal path parameters were transmitted instead. All filters run at 5 Hz.

1) Follower's estimate of Leader's path parameters: The leader's path parameters are broadcast every 5 s. Each follower should run its own filter to estimate these parameters in between samples, at a sufficiently high rate for control purposes. To this end, we used a Kalman filter, based on a discretized version of the model:

$$\frac{d}{dt}\begin{bmatrix} V_L \\ \chi_L \\ \dot{\chi}_L \end{bmatrix} = \begin{bmatrix} 0 \\ \dot{\chi}_L \\ 0 \end{bmatrix} \tag{57}$$

$$\boldsymbol{y} = \boldsymbol{x} \tag{58}$$

2) Currents and Follower-Leader relative position: Two other signals needed by the controllers are $\boldsymbol{p} - \boldsymbol{p}_L$ and $\boldsymbol{V_c}$. We estimate them with a Kalman filter, obtained from a discretized version of the model consisting of (59) and (61).

$$\dot{\boldsymbol{x}} = \frac{d}{dt}\begin{bmatrix} \boldsymbol{p} - \boldsymbol{p}_L \\ \boldsymbol{V}_c \end{bmatrix} = \begin{bmatrix} R(\psi)\begin{bmatrix} u \\ 0 \end{bmatrix} + \boldsymbol{V}_c - \dot{\boldsymbol{p}}_L \\ 0 \end{bmatrix} \tag{59}$$

$$\boldsymbol{y} = \begin{bmatrix} \boldsymbol{y}_{USBL} \\ \boldsymbol{y}_{DVL} \end{bmatrix} = \begin{bmatrix} \boldsymbol{p} - \boldsymbol{p}_L \\ \dot{\boldsymbol{p}} \end{bmatrix} \tag{60}$$

$$\boldsymbol{y}' = \begin{bmatrix} \boldsymbol{p} - \boldsymbol{p}_L \\ \boldsymbol{V}_c \end{bmatrix} = \boldsymbol{x} \tag{61}$$

where ψ, u and $\dot{\boldsymbol{p}}_L$ are inputs, and $\dot{\boldsymbol{p}}_L$ is obtained from the parameters estimated by the filter described above. This formulation assumes that the vehicle carries a DVL, capable of measuring $\dot{\boldsymbol{p}}$. This is not generally the case with the MEDUSAs, but the system is observable even if no DVL measurements are available. The measurement $\boldsymbol{y}'_{DVL} = \boldsymbol{y}_{DVL} - R(\psi)[u,\ 0]^T = \boldsymbol{V_c}$ was used instead of the original $\boldsymbol{y}_{DVL}$ so that the outputs coincide with the states.

Figure 7 illustrates the structure of the estimation and control blocks running in both underwater followers of the upper segment (GCV and LSV).

Remark 2. Although u is an input to the filter, the MEDUSAs currently have no onboard sensor than can measure the true surge speed. Instead, a static equation is used to determine an approximate value of u from the thruster RPMs. This implies that the acceleration/deceleration dynamics of the vehicle in the x_B axis are ignored, and has some practical consequences that will be exposed in the results.

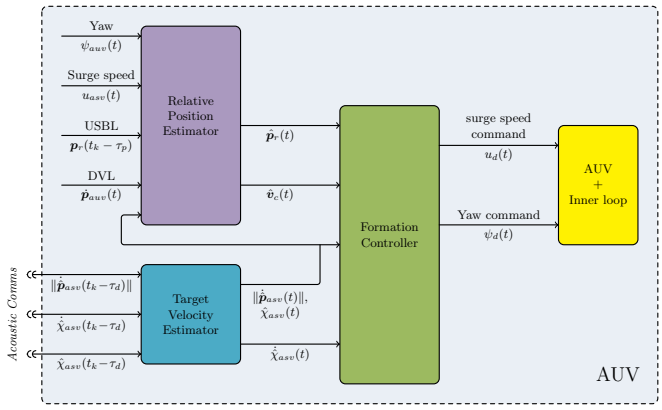

Figure 7: Estimation and control in underwater followers of the upper segment (drawn in collaboration with Mohammadreza Bayat).

VI. Results

We now show results of one computer-simulated mission and a five-vehicle mission at sea, on the Azores MORPH trials. The computer-simulated mission consists of a lawnmower with three upper segment vehicles and two lower segment. The nominal parameters of the trajectory of the leader are a velocity of 0.5 m/s and turn radius of 10 m. The formation parameters are $\boldsymbol{\delta} = (10, 0)$ for vehicle 2, $\boldsymbol{\delta} = (20, 0)$ for vehicle 3, ${}^M\boldsymbol{p}_d = (0, -2)$ for vehicle 4 and ${}^M\boldsymbol{p}_d = (0, 2)$ for vehicle 5 (see Figure 8. The controller parameters are $\delta = -0.02$ m, $k_x = 0.5$, $k_y = 0.5$, $n = 5$, $k_u = 10$, $k_r = 10$. The mission starts near the top left corner of the trajectory plots. For readability, the plots do not show the trajectory of the leader, the tracking errors or the current estimates for the upper segment vehicles.

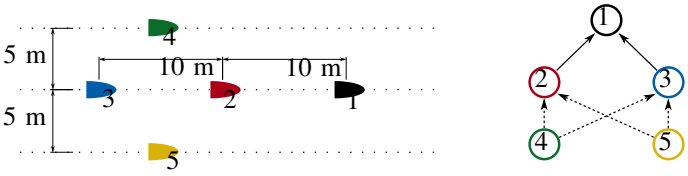

Figure 8: Nominal formation geometry and leader-follower topology for this simulation.

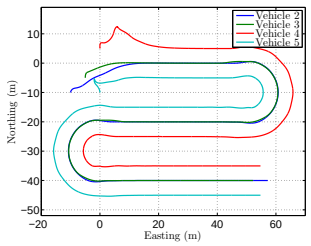

(a) Trajectories

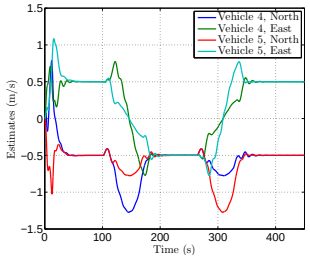

(b) Estimate: target velocity minus current $\dot{\boldsymbol{p}}_d - \boldsymbol{V}_c$

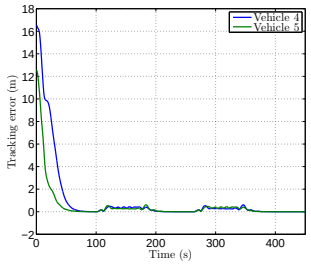

(c) Norm of tracking errors

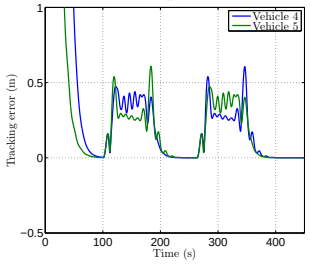

(d) Magnified norm of tracking errors

Figure 9: Results on simulated mission.

The estimates of $\dot{\boldsymbol{p}}_d - \boldsymbol{V_c}$ converge to the true values during straight segments; when turning, the sway and the acceleration of the virtual target perturb the estimates. The tracking error converges to zero in straight segments but is perturbed by sway and acceleration of the virtual target in turns; it still remains bounded as expected.

Figure 10 shows the results of the upper segment vehicles in a mission performed at the MORPH trials in Horta, Azores. Five vehicles were involved; three MEDUSAs played the role of MORPH upper segment vehicles, running the controllers and estimators as described in Chapter V. The position error is again around 1 m along x_B: possibly due to the fact that in between samples the position is estimated with a Kalman filter, which is naturally affected by an error. With

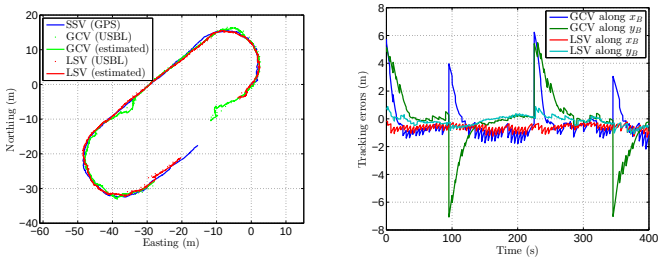

(a) Trajectories

(b) Tracking errors

Figure 10: Results on trials with MEDUSAs in the Azores.

the MEDUSAs this problem is aggravated: because the filter input u is an approximation of the real surge speed based on the thruster RPMs, as mentioned in Chapter V, the vehicle is considered to accelerate/decelerate instantaneously. When the controller acts to reduce a position error, the RPMs vary almost immediately, even though the acceleration or deceleration is not instantaneous. The filter then produces optimistic estimates of the position error along x_B, producing the sawtooth-like shape seen in Figure 10b.

VII. Conclusion and Future Steps

This thesis focused on the problem of formation control of autonomous underwater vehicles, motivated by multiple application scenarios. Only one leader vehicle was assumed to have a-priori knowledge of the mission to be executed. The problem of controlling the followers so as to move in a formation was first tackled using tools from nonlinear systems theory. It was divided into three main tasks: driving a follower vehicle to a virtual target (motion control), generating the virtual target according to the formation objectives (path-generation), and estimating currents or virtual target velocities (estimation). The path-generation and estimation tasks were analysed for two different scenarios: formation control with relative position measurements, and with range-only measurements. Stability and boundedness results were obtained from this analysis. Implementation of the controllers and estimators and an appropriate information flow strategy were described. Simulations results illustrate properties expected from the theoretical analysis. Real trials were conducted in Lisbon, Girona and the Azores, as part of the MORPH project, demonstrating the performance of the estimators and controllers in sea trials.

We now discuss briefly some problems that warrant further research. Although appreciated for their simplicity, leader-follower formations have well-known drawbacks concerning over-reliance on a single vehicle; extending the results in this thesis to *general formation topologies* is a difficult task under the general framework of nonlinear system theory, but could have significant impact, especially if practical limitations inherent to underwater communication and navigation systems are taken into account. In the scope of the MORPH project, one of the initial goals was that the system should perform better than a single vehicle in challenging environments, through inter-vehicle cooperation. During the next months, the research work will be focused on *controlling a vehicle formation in a fully three-dimensional space*, possibly by including formation operators such as tilt and scale. If successful, this would have considerable impact by paving the way for AUVs to be used in mapping and surveying of environments such as negative-slope walls. Finally, with further developments in acoustic communications and the recent introduction of optical systems, which support much higher bandwidths, the cooperation may shift from the motion level to the level of autonomous decision-making in a not too distant future. This would significantly increase the autonomy of the formation, allowing missions to be carried out without human supervision.

References

[1] J. Kalwa, M. Carreiro-Silva, F. Tempera, J. Fontes, R. Santos, M.-C. Fabri, L. Brignone, P. Ridao, A. Birk, T. Glotzbach, M. Caccia, J. Alves, and A. Pascoal, "The MORPH concept and its application in marine research," in *OCEANS - Bergen, 2013 MTS/IEEE*, June 2013, pp. 1–8.

[2] A. Aguiar and J. Hespanha, "Trajectory-tracking and path-following of underactuated autonomous vehicles with parametric modeling uncertainty," *IEEE Transactions on Automatic Control*, vol. 52, no. 8, pp. 1362–1379, 2007.

[3] R. Ghabcheloo, A. P. Aguiar, A. Pascoal, C. Silvestre, I. Kaminer, and J. Hespanha, "Coordinated path-following in the presence of communication losses and time delays," *SIAM Journal on Control and Optimization*, vol. 48, no. 1, pp. 234–265, 2009.

[4] R. Olfati-Saber and R. M. Murray, "Distributed cooperative control of multiple vehicle formations using structural potential functions," in *IFAC World Congress*, 2002, pp. 346–352.

[5] W. B. Dunbar and R. M. Murray, "Model predictive control of coordinated multi-vehicle formations," in *Decision and Control, 2002, Proceedings of the 41st IEEE Conference on*, vol. 4. IEEE, 2002, pp. 4631–4636.

[6] J. P. Desai, J. Ostrowski, and V. Kumar, "Controlling formations of multiple mobile robots," in *Robotics and Automation, 1998. Proceedings. 1998 IEEE International Conference on*, vol. 4. IEEE, 1998, pp. 2864–2869.

[7] J. M. Soares, A. P. Aguiar, A. M. Pascoal, and M. Gallieri, "Triangular formation control using range measurements: An application to marine robotic vehicles," in *3rd IFAC Workshop on Navigation, Guidance and Control of Underwater Vehicles (NGCUV 2012)*, no. EPFL-CONF-180991, 2012.

[8] J. M. Soares, A. P. Aguiar, A. M. Pascoal, and A. Martinoli, "Joint ASV/AUV range-based formation control: Theory and experimental results," in *Robotics and Automation (ICRA), 2013 IEEE International Conference on*. IEEE, 2013, pp. 5579–5585.

[9] ——, "Design and implementation of a range-based formation controller for marine robots," in *ROBOT2013: First Iberian Robotics Conference*. Springer, 2014, pp. 55–67.

[10] F. Rego, J. M. Soares, A. Pascoal, A. P. Aguiar, and C. Jones, "Flexible triangular formation keeping of marine robotic vehicles using range measurements," 2014.

[11] F. I. Vanni, "Coordinated Motion Control of Multiple Autonomous Underwater Vehicles," Master's thesis, 2007.

[12] The Society of Naval Architects and Marine Engineers (SNAME), "Nomenclature for treating the motion of a submerged body through a fluid," New York, Tech. Rep., 1950.

[13] T. I. Fossen, *Guidance and control of ocean vehicles*. Wiley New York, 1994, vol. 199, no. 4.

[14] H. Khalil, *Nonlinear Systems*. Prentice Hall PTR, 2002.

[15] A. P. Aguiar and A. M. Pascoal, "Dynamic positioning and way-point tracking of underactuated AUVs in the presence of ocean currents," *International Journal of Control*, vol. 80, no. 7, pp. 1092–1108, 2007.